Pergamon

Int. J. Solids Structures Vol. 34, No. 27, pp. 3491–3515, 1997

0020–7683/97 $17.00 + .00

PII: S0020–7683(96)00212–0

MODELLING THE INELASTIC CYCLIC BEHAVIOUR OF A BRACING MEMBER FOR WORK-HARDENING MATERIAL

ALEXANDER M. REMENNIKOV and WARREN R. WALPOLE
Department of Civil Engineering, University of Canterbury, Private Bag 4800, Christchurch, New Zealand

(*Received* 20 *March* 1996; *in revised form* 26 *September* 1996)

Abstract—This paper presents an incremental analytical model for theoretically predicting the strain hardening hysteretic behaviour of a steel brace member subjected to cyclic loading. The model consists of a pin-ended bracing member with a plastic hinge at midspan. Braces with other end conditions are handled using the effective length concept. An incremental solution procedure is herein employed where the incremental axial force dP is related to the incremental axial deformation $d\delta$ by means of a tangent stiffness coefficient K_t. Stepwise regression analysis is used to approximate the plastic conditions for the steel Universal Column (UC) section. Different cross section shapes of a bracing member can be accounted for by specifying the different yield surface approximations. Several simple one-surface type hardening rules are employed to evaluate the effect on the analytical prediction of a steel bracing cyclic behaviour. The analytical results are compared with available experimental data on actual brace members, confirming the validity of the analytical model developed for practical use. The proposed model has been incorporated into an inelastic dynamic frame analysis program to evaluate the inelastic seismic response of the braced steel structures.

1. INTRODUCTION

The seismic performance of steel structures is highly dependent on the hysteretic behaviour of their members. The assessment of this behaviour can be achieved by means of experimental tests and by the use of analytical models that take into account the phenomena involved in a non-linear response. The brace members are recognised to be a main source of earthquake energy dissipation in the concentrically braced steel frames. However, the cyclic inelastic behaviour of such braces is quite complex. The physical phenomena, which influence the hysteretic behaviour of the brace members, are the buckling of an element, yielding of material, local buckling, Bauschinger effect, etc. To better predict the seismic response of the braced frame structures, the efficient and versatile analytical brace model must be developed to allow the computer study to be made on large structural systems. Experimental results (Black *et al.*, 1980) have helped to identify the important physical responses of braces subjected to cyclic inelastic buckling. Along with the formation of plastic hinges, plastic axial deformation was found to contribute significantly to the total axial deformation of braces with low slenderness ratios ($kL/r < 60$) and to have a major effect on the magnitude of midspan lateral deflections. Plastic axial deformation also influences the behaviour of members with intermediate to high slenderness ratios ($kL/r > 60$). In experiments, the hysteretic growth in specimens was observed, which can be attributed to plastic axial deformation in the hinges that occurs during tension loading while restraightening a buckled member.

Recently, several analytical models have been developed to represent the cyclic behaviour of steel elements. These models can be divided into three types of brace modelling techniques: finite elements, phenomenological brace models and physical theory models.

The finite element approach generally subdivides a brace longitudinally into a series of elements. Each of these may be subdivided again into a number of elements. In this approach, the cross section geometry and material properties of each element are defined, and a large displacement analysis of the complete system is performed. The advantages of the finite element approach is its general applicability to many types of problems, and that

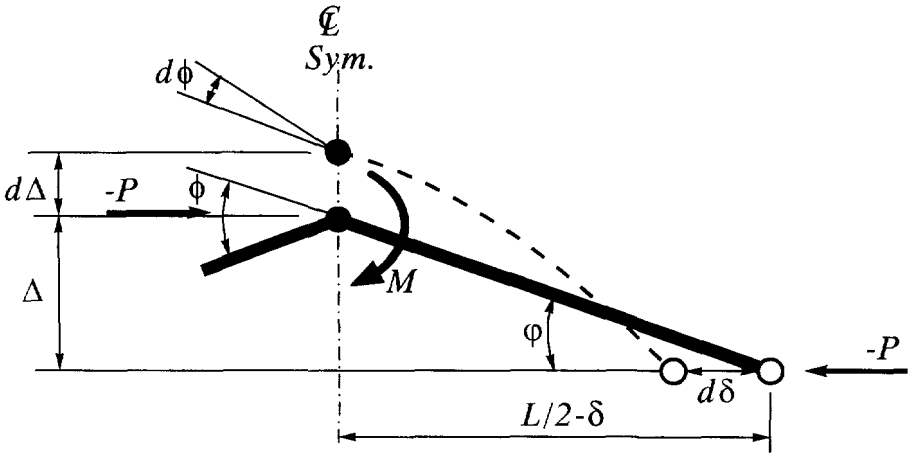

Fig. 1. Deformed shape of a brace member.

only the member geometry and material properties need to be defined. Kayvani and Barzegar (1996) have recently employed this approach for modelling the seismic behaviour of an offshore platform. A limitation of this approach is that it is computationally expensive.

Phenomenological models are based on simplified hysteretic rules which only mimic the observed force–displacement curves of a brace member. Models of this type have been developed by Higginbotham (1973), Nilforoushan (1973), Singh (1977), Jain and Goel (1978) and Maison and Popov (1980). Accurate representation of member cyclic behaviour is possible with phenomenological models when the shape of the hysteretic loops is known. The use of such models requires specification of numerous empirical input parameters for each element analysed.

Physical theory models incorporate simplified theoretical formulations based on physical considerations that allow the cyclic inelastic behaviour to be computed. Unlike the phenomenological models, the input data for physical theory models is based on the material properties and geometric properties of a member. Some of the models are reviewed here to give a better understanding of the various approaches towards the formulation of physical theory models.

Physical theory models usually consist of elastic beam segments with an elastoplastic cell representing the assumed location of a plastic hinge (Fig. 1). Three types of material models have been employed: (1) the elasto-perfectly plastic; (2) the bi-linear stress–strain relationship; and (3) the piecewise linear stress–strain relationship. Some researchers (Nonaka, 1973; 1977; Gugerli and Goel, 1982) formulated a general elastic–plastic solution for the hysteretic behaviour of a prismatic bar subjected to repeated axial loading. They assumed the elasto-perfectly plastic material behaviour in the analysis under the combined action of axial force and bending moment. They solved the beam-column equation directly, obtaining sine curves for the deflected shape of the beam segments under compression and hyperbolic sine curves for beam segments under tension. Ikeda proposed a refined physical theory brace model (Ikeda and Mahin, 1984) which was based on Gugerli's formulation. The changes made to Gugerli's model were to replace the initial modulus of elasticity E by the tangent modulus of elasticity E_t so as to better replicate material non-linearities.

Shibata (1982) derived a closed-form solution for a bar of ideal I-section with a bi-linear stress–strain relationship. For a bar of arbitrary cross section with a piecewise linear stress–strain relationship, an incremental load–displacement relationship was obtained in an analytical form. His model was composed of an elastic–plastic spring and two straight segments. In the actual calculation, the midsection should be divided into a finite number of strip elements, in order to calculate the restoring moment and axial force in the spring for the assumed material behaviour. So, the application of this procedure is limited to bracing members with special cross section shapes. A similar model has been proposed by Ballio and Perotti (1987) assuming a bi-linear material model. Although the method used by Shibata, and Ballio and Perotti seems attractive because it is possible to account for the

gradual spread of plasticity over the critical cross section and to take into consideration the local buckling effects, it requires solving non-linear equations at each fibre so many times that it becomes inappropriate for the dynamic analysis of structural systems with large numbers of bracing members. Furthermore, the formulations of the above models express axial displacement as a function of an axial force. Thus, these models necessitate additional iterations in order to estimate the value of axial force for a given displacement. Moreover, these formulations are inconsistent with the finite element analysis procedure used to analyse the dynamic response of braced structures.

The refined physical theory brace model (Ikeda and Mahin, 1984) was chosen for further development of the incremental physical theory brace model (Remennikov and Walpole, 1995). The incremental brace model is compatible with the conventional dynamic analysis computer programs and incorporates refinements from recent experimental work.

Tests carried out in the Civil Engineering Laboratory at the University of Canterbury on a series of struts (Leowardi, 1994; Walpole, 1995) revealed some limitations of available physical brace models which can be attributed to the material models assumed in previously developed approaches. Experimental results (Ikeda and Mahin, 1984; Leowardi, 1994) have proved that the struts may exhibit significant strain hardening and strain softening during later cycles of loading. Therefore, it was decided to improve an incremental physical theory brace model (Remennikov and Walpole, 1995) with better implementation of the Bauschinger effect so as to enable the model to represent the strain hardening and strain softening effects. Bearing in mind that the proposed model was intended to be incorporated into the inelastic dynamic analysis program in order to evaluate the response of the braced systems with a large number of bracings, a number of simple one-surface type hardening rules was studied for the sake of computer efficiency. Also, the one-surface type hardening models required less empirical parameters to be specified from tests than the two- or multiple-surface type hardening models (Mroz, 1983; Tseng and Lee, 1983; Jiang and Sehitoglu, 1996). The hardening rules employed were those of Prager (1956); Phillips and Lee (1977) and Ziegler (1959), and their combinations, with the isotropical hardening model. Some details on the inelastic behaviour of a brace member under cyclic loading are presented in the next section.

2. CYCLIC BEHAVIOUR OF A BRACE MEMBER

2.1. *Zone definition*

Figure 2 shows the typical hysteretic behaviour of a steel member when subject to axial cyclic loading. It is common to divide a cycle into a set of zones, corresponding to different behavioural characteristics. Following the approach of Ikeda and Mahin (1984), a cycle is divided into four general categories for a better representation of cyclic behaviour: the elastic zone, plastic zone, elastic buckling zone and yield zone. The terms "elastic" and "plastic" correspond to the state of the plastic hinge, while the term "yield" is associated with the state of the beam segments. After that, the elastic zone is subdivided into the elastic shortening (both member length and axial load decrease) and the elastic lengthening zone (both member length and axial load increase). Finally, the elastic shortening, elastic lengthening and plastic zones are further subdivided into the zones in compression and those in tension. As a result, the eight zones are incorporated to properly define the axial force–deformation curve, axial force–plastic hinge moment curve and axial force–plastic hinge rotation curve (Fig. 2). The detailed description of each zone is given elsewhere (Remennikov and Walpole, 1996). Within the scope of the paper, the plastic behaviour of a brace is briefly discussed.

Zone P1 is the plastic zone in compression. In this state, a yield hinge has been formed at the centre, and an increasing deflection is accompanied by the large rotation and plastic axial deformation at the hinge. It is evident that the equilibrium of the half member is maintained only under decreasing compression. In this zone, the P–M curves tend to follow the theoretical fully plastic interaction curve. Zone P2 is the plastic zone in tension. Elastic behaviour ceases to continue to a point at which the yield limit is reached, with positive axial load P. Plastic action again takes place with the stress point on the yield surface. The

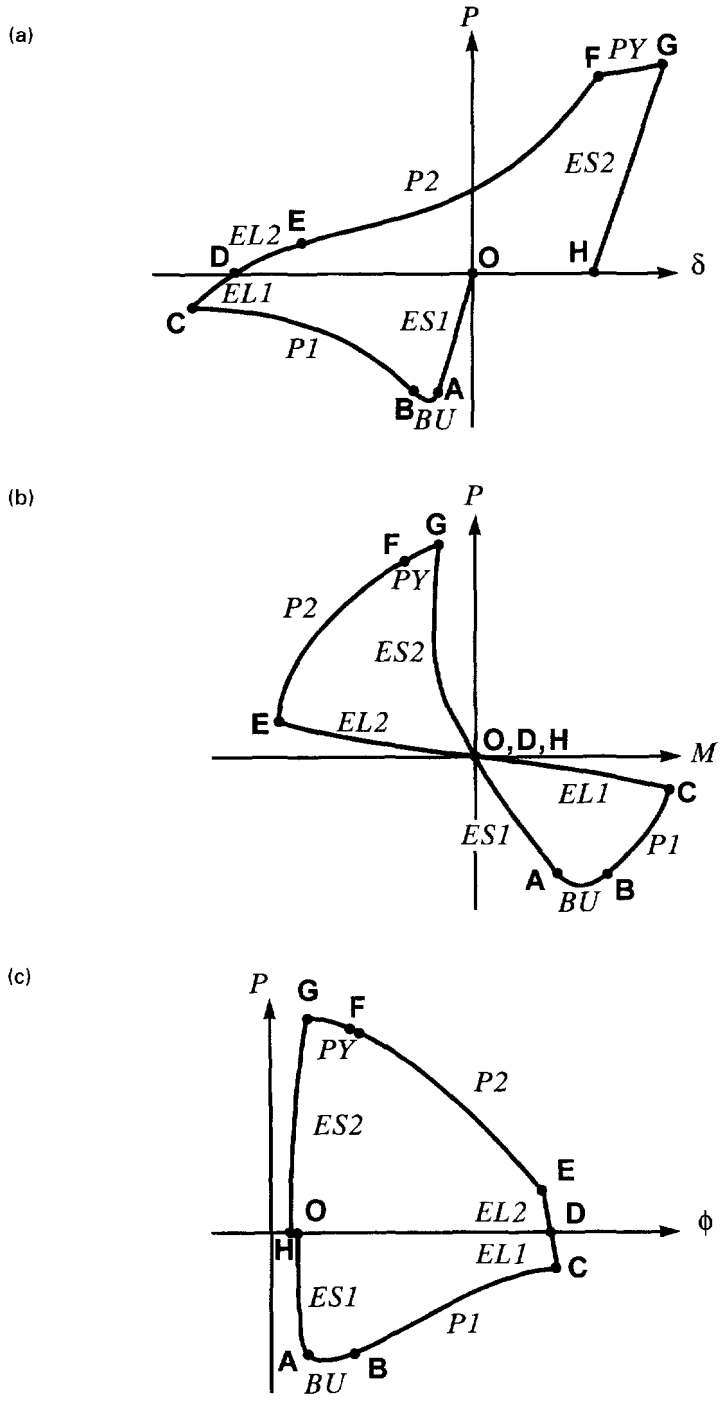

Fig. 2. Definition of different zones: (a) P–δ curve; (b) P–M curve; (c) P–ϕ curve.

plastic rotation as well as lateral deflection decreases. The P–Δ moments, where Δ denotes the lateral deflection at midspan, start to reduce as the brace straightens up. To sustain yielding, the tensile axial load must increase. The brace model presented takes into account the strain-hardening material behaviour in two plastic zones P1 and P2.

2.2. *Model of tangent modulus history*

As an experimental fact, the tangent modulus of elasticity deteriorates significantly during inelastic cyclic. The tangent modulus history derived from the 150UC30 stub column

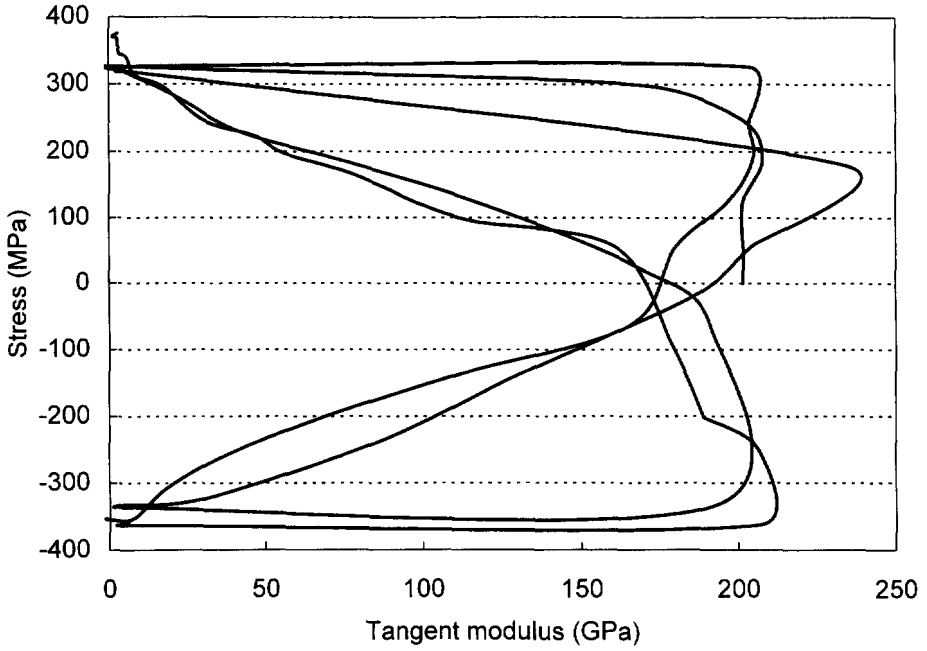

Fig. 3. Tangent modulus history.

cyclic test is shown in Fig. 3. Based on the experimental data, an empirical model was formulated (Ikeda and Mahin, 1984) for the normalised tangent modulus $e = E_t/E$ as a function of the normalised axial force $p = P/P_y$. Figure 4 shows two pairs of linear idealisation curves utilised to define the decrease and increase patterns, as well as the relation of these curves to the zones of a brace cyclic behaviour. The values of four parameters e_1, e_2, e_3 and e_4 must be selected to account for available experimental data on the tangent modulus

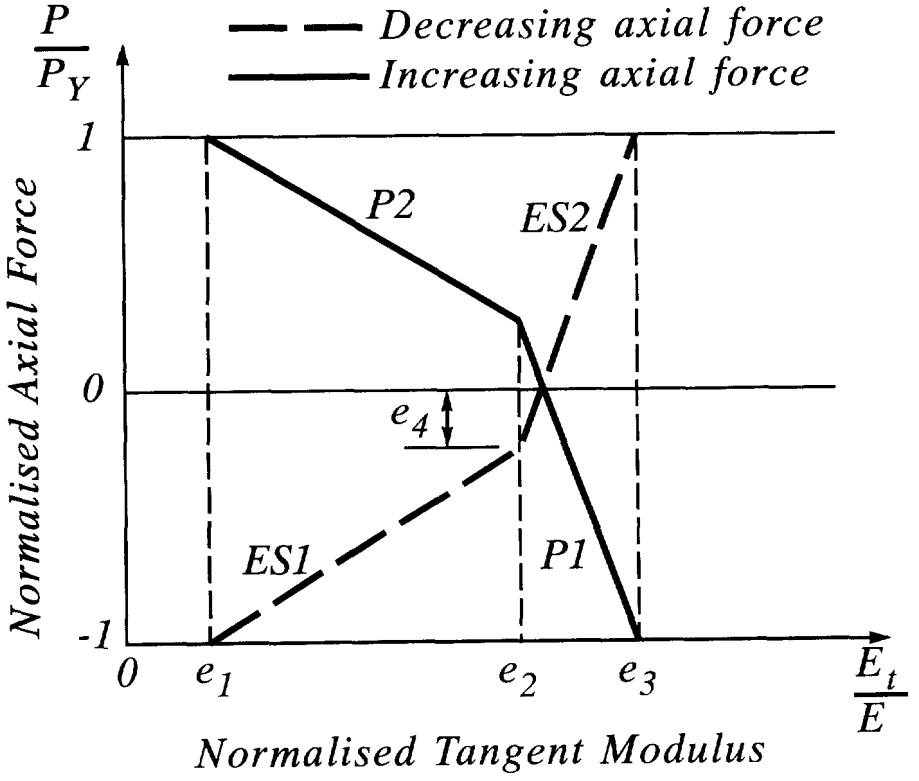

Fig. 4. Tangent modulus empirical model.

of elasticity. These idealisation curves are used hereinafter to describe the changes in the tangent modulus E_t at different stages of a brace inelastic behaviour.

3. INCREMENTAL PHYSICAL THEORY BRACE MODEL

The physical model for a pin-ended brace member with plastic hinge at midspan is shown in Fig. 1. The member is loaded with an axial load P, that causes an internal plastic hinge moment M, an axial deformation δ and plastic hinge rotation Φ.

The axial force–plastic hinge moment interaction relationship (Appendix) is used to define the fully plastic state in the centre hinge. States of force inside the interaction surface are assumed elastic; deformation hardening occurs outside this surface. When the current yield surface is reached, the plastic flow rule (Drucker, 1960) is used to define the orientation of the incremental plastic deformation vector.

For simplicity, basic equations are developed for the right half of a brace member shown in Fig. 1. The deflected shape of the brace can be obtained by solving the basic beam-column equation (Chen and Atsuta, 1977). Then, the plastic hinge moment–plastic hinge rotation relationship can be established as:

$$M = \gamma(v)\frac{E_t I}{L}\phi = \gamma(v)(E_t I)\Phi \tag{1}$$

where $\Phi = \phi/L$, parameter $v^2 = |P|L^2/(E_t I)$ and $\gamma(v)$ is defined as follows:

$$\gamma(v) = \begin{cases} \dfrac{v}{2}\tan\dfrac{v}{2} & \text{if } P < 0 \\ -\dfrac{v}{2}\tanh\dfrac{v}{2} & \text{if } P > 0 \end{cases}. \tag{2}$$

Hence, it follows that the plastic hinge rotation is expressed as:

$$\Phi = (\gamma(v)E_t I)^{-1} M. \tag{3}$$

The model formulation assumes elastic axial and flexural deformations along the length of the brace, and plastic axial and flexural deformations concentrated in the plastic hinge. The total axial deformation increment, considering second-order effects, may be expressed as:

$$\mathrm{d}\delta = \mathrm{d}\delta_e + \mathrm{d}\delta_g + \mathrm{d}\delta_p + \mathrm{d}\delta_{ty} \tag{4}$$

where δ_e is the elastic axial deformation; δ_g is the geometric shortening deformation; δ_p is the plastic hinge deformation; and δ_{ty} is the tensile yield deformation. The elastic axial deformation increment, $\mathrm{d}\delta_e$, is expressed as:

$$\mathrm{d}\delta_e = \{E_t(P)A\}^{-1}\,\mathrm{d}P \tag{5}$$

where A is the cross-sectional area.

Geometric shortening deformation, δ_g, of a brace member may be expressed as follows:

$$\begin{aligned} \delta_g &= -\frac{1}{2}\int_0^1 (\Delta'(x))^2\,\mathrm{d}x \\ &= -h_1(v)\phi^2 = -h_1(v)\Phi^2 L^2 \end{aligned} \tag{6}$$

where

$$h_1(v) = \begin{cases} \dfrac{\dfrac{\sin v}{v} + 1}{16\cos^2\dfrac{v}{2}} & \text{if } P < 0 \\ \dfrac{\dfrac{\sinh v}{v} + 1}{16\cosh^2\dfrac{v}{2}} & \text{if } P > 0 \end{cases}. \tag{7}$$

Eqn (6) can be introduced in an incremental form as follows:

$$\mathrm{d}\delta_g = \langle S\rangle L^2 \left[\frac{\mathrm{d}h_1(v)}{\mathrm{d}v}\frac{\mathrm{d}v}{\mathrm{d}P}\Phi_i^2 + 2h_1(v)\Phi_i\frac{\mathrm{d}\Phi(P_i)}{\mathrm{d}P}\right]\mathrm{d}P \tag{8}$$

in which subscript i denotes the values of forces P, moments M and rotation Φ before the deformation increment $\mathrm{d}\delta$ takes place, and

$$\langle S\rangle = \begin{cases} -1 & \text{if } P < 0 \\ +1 & \text{if } P > 0 \end{cases}. \tag{9}$$

A method of evaluating the derivatives $\mathrm{d}h_1(v)/\mathrm{d}v$, $\mathrm{d}v/\mathrm{d}P$ and $\mathrm{d}\Phi/\mathrm{d}P$ is given further on.

The plastic hinge deformation increment, $\mathrm{d}\delta_p$, is evaluated on the basis of the plastic flow rule, resulting from Drucker's Postulate (Drucker, 1960). It states that the incremental plastic deformation vector must be in the direction of the outward normal to the yield surface f at the corresponding stress point, i.e.

$$\begin{aligned} \mathrm{d}\delta_p &= \mathrm{d}\lambda f_{,P} \\ \mathrm{d}\Phi_p &= \mathrm{d}\lambda f_{,M} \end{aligned} \tag{10}$$

where $f_{,P}$ and $f_{,M}$ are the derivatives of yield function f with respect to P and M. Dividing the first line by the second line in eqn (10), one can arrive at the following expression for $\mathrm{d}\delta_p$

$$\mathrm{d}\delta_p = \frac{f_{,P}}{f_{,M}}\frac{\mathrm{d}\Phi_p}{\mathrm{d}P}\mathrm{d}P. \tag{11}$$

The derivatives $f_{,P}$ and $f_{,M}$ can be easily calculated as soon as the explicit form of the yielding surface or axial force–moment interaction curve is established. For the yield surface details see the Appendix.

Finally, eqns (4), (5), (8) and (11) can be combined as

$$\mathrm{d}P = K_t\,\mathrm{d}\delta \tag{12}$$

where

$$K_t = \frac{E_tA}{1 + \langle S\rangle(E_tA)L^2\left\{\dfrac{\mathrm{d}h_1(v)}{\mathrm{d}v}\dfrac{\mathrm{d}v}{\mathrm{d}P}\Phi_i^2 + 2h_1(v)\Phi_i\dfrac{\mathrm{d}\Phi_p}{\mathrm{d}P}\right\} + (E_tA)\dfrac{f_{,P}}{f_{,M}}\dfrac{\mathrm{d}\Phi_p}{\mathrm{d}P}}. \tag{13}$$

The tangent stiffness coefficient K_t defines the inelastic brace properties for an incremental solution. Equation (12) can be used to find the incremental axial force when the state is on

the yield surface and is loaded inelastically. The plastic hinge moment increment can be calculated from the consistency condition for a work hardening material:

$$df = 0. \tag{14}$$

When the loading is elastic, $d\delta_p$ is equal to zero, eqn (12) may be simplified as:

$$dP = (E_t A)\left[1 + \langle S\rangle (E_t A) L^2 \left\{\frac{dh_1(v)}{dv}\frac{dv}{dP}\Phi_i^2 + 2h_1(v)\Phi_i\frac{d\Phi_p}{dP}\right\}\right]^{-1} d\delta. \tag{15}$$

This general equation can be used to get the incremental forces when the state is inside the yield surface, or when unloading from the yield surface.

From eqns (5)–(15), stiffness and state determination algorithms for a computer model can be formulated. The incremental forces can be solved in terms of the incremental deformations by use of either eqns (12) or (15).

4. PLASTICITY MODEL IN STRESS–RESULTANT SPACE

4.1. *Assumptions*

A plasticity model for the stress resultant (force) and strain (axial and flexural deformations) relationship of a steel section is developed. The incremental theory is employed in developing constitutive equations for work-hardening materials (Chen and Han 1988). This type of formulation relates the increment of plastic strain components $d\{\varepsilon^p\}$ to the state of stress and stress resultant increment $d\{F\}$. Basic assumptions used in the development of the incremental theory of work-hardening plasticity include:

- The existence of an initial stress resultant yield surface which defines the elastic limit of the material.
- The hardening rule which describes the evolution of subsequent yield surfaces.
- The flow rule which is related to a yield function and defines the direction of the incremental plastic strain vector.

4.2. *Basic approach*

Consider a single yield surface that is a function of stress resultant $\{F\}$. The stress resultant consists of two forces: P and M, where P is the axial force, and M is the plastic hinge moment. Then, $\{F\}$ is defined as follows

$$\{F\} = [P, M]^T. \tag{16}$$

According to the incremental theory of work-hardening plasticity, a general constitutive equation for an elastic–plastic work-hardening material will be derived in the form of

$$d\{F\} = \mathbf{D}^{ep}\, d\{\varepsilon\} \tag{17}$$

where $\mathbf{D}^{ep}$ is the elastoplastic stiffness matrix, which is a function of stress state and loading history. For a given stress state and loading history, eqn (17) gives the stress resultant increment $d\{F\}$ for a given deformation increment $d\{\varepsilon\}$ which constitutes a plastic loading. This equation is needed in a numerical analysis of plasticity, such as a finite element analysis.

It is generally postulated as an experimental fact, that yielding can occur only if the stresses satisfy the general yield criterion

$$f(\{F\}, \{\alpha\}, \kappa) = 0 \tag{18}$$

where $\kappa = \kappa(\varepsilon^p)$ is an isotropic hardening parameter that depends on the plastic strain

increment; and $\{\alpha\}$ is the vector of coordinates of centre of the loading surface which are also dependent on deformation increment. This yield condition can be visualised as a surface in n-dimensional space of stress resultant, with the position of the surface dependent on the values of the hardening parameters κ and $\{\alpha\}$.

When the current yield surface f is reached, the material is in a state of plastic flow upon further loading. The flow rule (Drucker, 1960) is defined as:

$$\mathrm{d}\{\varepsilon^{\mathrm{p}}\} = \mathrm{d}\lambda \frac{\partial f}{\partial \{F\}} \tag{19}$$

where $\mathrm{d}\lambda$ is a positive scalar function that will vary throughout the history of the straining process. The gradient of the loading surface $\partial f/\partial\{F\}$ defines the direction of the plastic strain increment vector $\mathrm{d}\{\varepsilon^{\mathrm{p}}\}$, while the magnitude of the vector is given by the loading parameter $\mathrm{d}\lambda$.

If $\{n\}$ denotes the unit normal to the loading surface f, then

$$\{n\} = \frac{\left\{\dfrac{\partial f}{\partial \{F\}}\right\}}{\left(\left\{\dfrac{\partial f}{\partial \{F\}}\right\}^{\mathrm{T}} \left\{\dfrac{\partial f}{\partial \{F\}}\right\}\right)^{1/2}} \tag{20}$$

where $(\partial f/\partial\{F\})^{\mathrm{T}} = (\partial f/\partial P, \partial f/\partial M)^{\mathrm{T}}$. In this case, the deformation plastic increment $\mathrm{d}\{\varepsilon^{\mathrm{p}}\}$ is defined in accordance with the normality principle as follows:

$$\mathrm{d}\{\varepsilon^{\mathrm{p}}\} = \{n\}\, \mathrm{d}|\varepsilon^{\mathrm{p}}| \tag{21}$$

where $\mathrm{d}|\varepsilon^{\mathrm{p}}|$ is the length of the plastic deformation vector.

4.3. *Incremental stress resultant–strain relations*

During the infinitesimal increment of stress resultant $\mathrm{d}\{F\}$, the strain increment is assumed to be decomposed into elastic and plastic components

$$\mathrm{d}\{\varepsilon\} = \mathrm{d}\{\varepsilon^{\mathrm{e}}\} + \mathrm{d}\{\varepsilon^{\mathrm{p}}\}. \tag{22}$$

The elastic strain increments are related to stress resultant increments by a symmetric elastic matrix $\mathbf{D}^*$. We can thus write eqn (22) incorporating the plastic relation (21) as:

$$\mathrm{d}\{\varepsilon\} = \mathbf{D}^{*-1}\, \mathrm{d}\{F\} + \mathrm{d}|\varepsilon^{\mathrm{p}}|\{n\} \tag{23}$$

or

$$\mathrm{d}\{F\} = \mathbf{D}^*(\mathrm{d}\{\varepsilon\} - \mathrm{d}\{\varepsilon^{\mathrm{p}}\}) = \mathbf{D}^*(\mathrm{d}\{\varepsilon\} - \mathrm{d}|\varepsilon^{\mathrm{p}}|\{n\}). \tag{24}$$

From the preceding equations, we can see that if we know the magnitude of the plastic deformation $\mathrm{d}|\varepsilon^{\mathrm{p}}|$, the constitutive relation is fully determined.

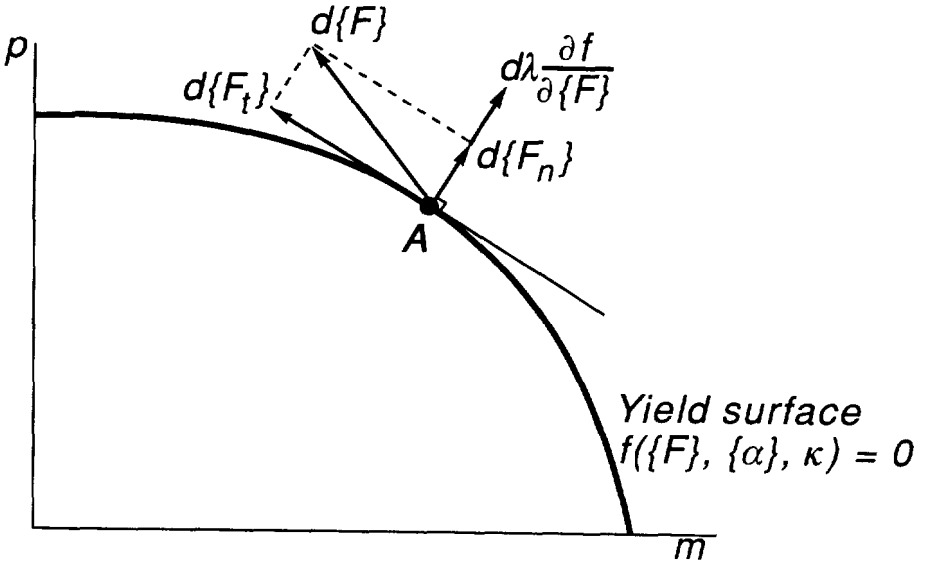

Fig. 5. Decomposition of stress resultant vector $d\{F\}$.

The magnitude of the plastic strain vector $d|\varepsilon^p|$ can be obtained on the grounds of the following geometric considerations (Fig. 5). Consider an element in a plastic state A, characterised by the stress resultant vector $\{F\}$. If we add to the current state $\{F\}$ an infinitesimal increment $d\{F\}$ (additional loading) and the angle between the vector $d\{F\}$ and $\{n\}$ is acute, additional plastic deformation will occur.

Let us decompose the vector $d\{F\}$ into two parts:

$$d\{F\} = d\{F_t\} + d\{F_n\} \tag{25}$$

where $d\{F_t\}$ and $d\{F_n\}$ are the tangent and normal components of vector $d\{F\}$ at the current point A.

In addition, we can state the following evident relations for these vectors:

$$\{n\}^T d\{F_t\} = 0, \tag{26}$$

$$d\{F_n\} = \{n\}^T d\{F\}\{n\} \tag{27}$$

and assume that the relationship between $d\{F_n\}$ and $d\{\varepsilon^p\}$ in the form similar to the elastic stress–strain relationship will be:

$$d\{F_n\} = \mathbf{D}^{pl} d\{\varepsilon^p\} \tag{28}$$

where $\mathbf{D}^{pl} = \text{diag}[(E_p A);(E_p I)]$ and E_p may be referred to as the plastic modulus, yet undetermined, which is a function of the current state of stress and hardening parameters. Bearing in mind eqns (21) and (25)–(28), we get

$$\{n\}^T d\{F\} = \{n\}^T d\{F_t\} + \{n\}^T d\{F_n\},$$

$$\{n\}^T d\{F\} = \{n\}^T \mathbf{D}^{pl} d\{\varepsilon^p\},$$

$$\{n\}^T d\{F\} = \{n\}^T \mathbf{D}^{pl}\{n\}\, d|\varepsilon^p|,$$

and, finally,

$$\mathrm{d}|\varepsilon^{\mathrm{p}}| = \frac{\{n\}^{\mathrm{T}}\,\mathrm{d}\{F\}}{\{n\}^{\mathrm{T}}\mathbf{D}^{\mathrm{pl}}\{n\}}. \tag{29}$$

From eqn (21), plastic strain increment takes the following form:

$$\mathrm{d}\{\varepsilon^{\mathrm{p}}\} = \frac{\{n\}^{\mathrm{T}}\,\mathrm{d}\{F\}}{\{n\}^{\mathrm{T}}\mathbf{D}^{\mathrm{pl}}\{n\}}\{n\} = \frac{\{n\}\{n\}^{\mathrm{T}}}{\{n\}^{\mathrm{T}}\mathbf{D}^{\mathrm{pl}}\{n\}}\mathrm{d}\{F\} \tag{30}$$

in which the unit normal to the loading surface at point A is defined by eqn (20).

4.4. *Loading/unloading criterion*

The loading/unloading criterion enables continuing plastic flow to be distinguished from elastic unloading. In the case of a multiaxial stress state, the loading/unloading criterion must be clearly specified. It is known that plastic flow occurs only when the stress point is on the loading surface and the stress incremental vector $\mathrm{d}\{\sigma\}$ is directed outward from the current elastic region.

An additional plastic deformation will occur if the angle between the vector $\mathrm{d}\{\sigma\}$ and $\{n\}$ is acute. That is, the continued loading occurs if

$$f = 0 \quad \text{and} \quad \{n\}\,\mathrm{d}\{\sigma\} > 0. \tag{31}$$

On the other hand, if these two vectors $\{n\}$ and $\mathrm{d}\{\sigma\}$ form an obtuse angle, unloading will occur. Thus, the unloading criterion is

$$f = 0 \quad \text{and} \quad \{n\}\,\mathrm{d}\{\sigma\} < 0. \tag{32}$$

However, eqns (31) and (32) can not be directly applied to the case of stress resultant space and cyclic behaviour of a brace member. This is because the brace member undergoes plastic deformation in such a way that the components of vector $\mathrm{d}\{F\}$ retain their positive values over the course of plastic loading both in tension and compression. This imposes an additional restriction on the relationship between the unit vector $\{n\}$ and the stress resultant vector $\mathrm{d}\{F\}$.

When in Zone P2, the requirement of positiveness of both components of vector $\mathrm{d}\{F\}$ is ensured by maintaining the direction of vector $\mathrm{d}\{F\}$ as shown in Fig. 6. In other words, an angle β_1 between a line $M = M_A$ and the direction $\mathrm{d}\{F\}$ must be within a range $0 < \beta_1 < \beta$, i.e.

$$0 < \tan\beta_1 < \tan\beta \tag{33}$$

where $\tan\beta_1 = \mathrm{d}M/\mathrm{d}P$ ($\mathrm{d}P$ and $\mathrm{d}M$ are the components of vector $\mathrm{d}\{F\}$). From Fig. 6, the angle β and consequently $\tan\beta$, can be found as follows:

$$\beta = \frac{\pi}{2} - \alpha;$$

$$\tan\beta = \tan\left(\frac{\pi}{2} - \alpha\right) = \frac{1}{\tan\alpha}; \tag{34}$$

but

$$\tan\alpha = -\frac{f_{,\mathrm{M}}}{f_{,\mathrm{P}}},$$

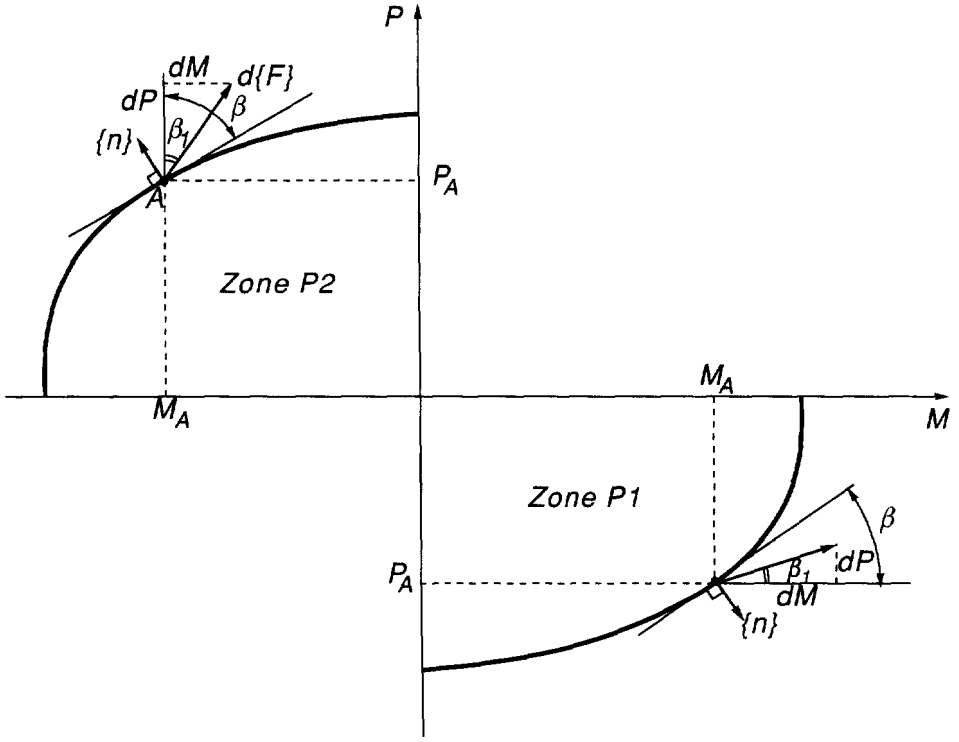

Fig. 6. Loading criterion for a brace member.

and

$$\tan\beta = -\frac{f_{,\mathrm{P}}}{f_{,\mathrm{M}}}.$$

From eqns (33) and (34), if follows that

$$0 < \frac{\mathrm{d}M}{\mathrm{d}P} < -\frac{f_{,\mathrm{P}}}{f_{,\mathrm{M}}}, \tag{35}$$

and

$$0 < \mathrm{d}M < -\mathrm{d}P\frac{f_{,\mathrm{P}}}{f_{,\mathrm{M}}}, \quad \mathrm{d}P > 0, \quad f_{,\mathrm{P}} > 0, \quad \text{and} \quad f_{,\mathrm{M}} < 0.$$

This equation can be considered as a sufficient condition of plastic flow within Zone P2 for a brace member.

Similarly, the loading criterion for Zone P1 can be derived from geometric consideration in Fig. 6. To ensure that plastic flow will occur in this zone, the following condition must be satisfied

$$0 < \tan\beta_1 < \tan\beta \tag{36}$$

where $\tan\beta_1 = \mathrm{d}P/\mathrm{d}M$. The angle β is determined, in this case, as follows

$$\beta = \frac{\pi}{2} - \alpha;$$

$$\tan\beta = \tan\left(\frac{\pi}{2} - \alpha\right) = \frac{1}{\tan\alpha}; \tag{37}$$

but

$$\tan\alpha = -\frac{f_{,\mathrm{P}}}{f_{,\mathrm{M}}},$$

and

$$\tan\beta = -\frac{f_{,\mathrm{M}}}{f_{,\mathrm{P}}}.$$

Equation (36) can be re-written in the following form:

$$0 < \frac{\mathrm{d}P}{\mathrm{d}M} < -\frac{f_{,\mathrm{M}}}{f_{,\mathrm{P}}}, \tag{38}$$

and

$$\mathrm{d}M > -\mathrm{d}P\frac{f_{,\mathrm{P}}}{f_{,\mathrm{M}}}, \quad \mathrm{d}P > 0, \quad f_{,\mathrm{P}} < 0, \quad \text{and} \quad f_{,\mathrm{M}} > 0.$$

Equation (38) establishes a sufficient condition of plastic flow within Zone P1.

4.5. *Evaluation of plastic hinge deformation for a work-hardening material*

Accomplishing the matrix operations in eqn (30), we get the following expressions for the incremental deformation vector components

$$\mathrm{d}\delta_{\mathrm{p}} = \frac{f_{,\mathrm{P}}(f_{,\mathrm{P}}\,\mathrm{d}P + f_{,\mathrm{M}}\,\mathrm{d}M)}{(E_{\mathrm{p}}A)f_{,\mathrm{P}}^2 + (E_{\mathrm{p}}I)f_{,\mathrm{M}}^2},$$

$$\mathrm{d}\Phi_{\mathrm{p}} = \frac{f_{,\mathrm{M}}(f_{,\mathrm{P}}\,\mathrm{d}P + f_{,\mathrm{M}}\,\mathrm{d}M)}{(E_{\mathrm{p}}A)f_{,\mathrm{P}}^2 + (E_{\mathrm{p}}I)f_{,\mathrm{M}}^2}. \tag{39}$$

Dividing the first equation in (39) by the second one, one can arrive at the expression for $\mathrm{d}\delta_{\mathrm{p}}$ which is identical to eqn (11).

The derivatives for Φ_{p} now take the following form:

$$\frac{\mathrm{d}\Phi_{\mathrm{p}}}{\mathrm{d}P} = \Phi_i\left[\frac{f_{,\mathrm{P}}/f_{,\mathrm{M}}}{M_i} - \frac{\dfrac{\mathrm{d}\gamma}{\mathrm{d}v}\dfrac{\mathrm{d}v}{\mathrm{d}P}}{\gamma(v_i)}\right]. \tag{40}$$

In this equation, the plastic hinge moment M_i, plastic hinge rotation Φ_i, and parameter v_i are calculated at the current stress point A.

From eqns (11) and (40), one can get the formula for $\mathrm{d}\delta_{\mathrm{p}}$

$$d\delta_p = \Phi_i \frac{f_{,P}}{f_{,M}} \left[\frac{f_{,P}/f_{,M}}{M_i} - \frac{\frac{d\gamma}{dv}\frac{dv}{dP}}{\gamma(v_i)} \right] dP. \tag{41}$$

This formula is used in the incremental physical theory brace model, which takes into account the work-hardening effect.

4.6. *Calculation of the plastic hinge moment increment for a work-hardening material*

From eqn (39), an increment of plastic hinge moment can be defined as follows:

$$dM = \left[(E_p A)\frac{f_{,P}}{f_{,M}} + (E_p I)\frac{f_{,M}}{f_{,P}} \right] d\delta_p - \frac{f_{,P}}{f_{,M}} dP > 0 \tag{42}$$

in which an axial force increment, dP, is determined from eqn (12); and a plastic deformation increment, $d\delta_p$, is defined above.

Equation (42) can be considered as the generalised expression for the plastic hinge moment increment, since, in the case of $E_p = 0$, it yields the consistency condition for a perfectly plastic material

$$dM = -\frac{f_{,P}}{f_{,M}} dP, \tag{43}$$

or

$$f_{,P}\, dP + f_{,M}\, dM = 0.$$

On the other hand, this equation can be shown to satisfy the loading criterion for a work-hardening material in the stress resultant space discussed in Section 4.2.

In Zone P1, where $f_{,P} < 0, f_{,M} > 0$, $d\delta_p < 0$ and $dP > 0$, it is evident that dM is positive for all points within Zone P1, and, therefore, eqn (42) gives:

$$dM - \left(-\frac{f_{,P}}{f_{,M}} dP \right) = \left[(E_p A)\frac{f_{,P}}{f_{,M}} + (E_p I)\frac{f_{,M}}{f_{,P}} \right] d\delta_p > 0 \tag{44}$$

or

$$dM > -\frac{f_{,P}}{f_{,M}} dP.$$

Similarly, in Zone P2, where $f_{,P} > 0, f_{,M} < 0$, $d\delta_p > 0$ and $dP > 0$, from eqn (42) one can get:

$$dM - \left(-\frac{f_{,P}}{f_{,M}} dP \right) = \left[(E_p A)\frac{f_{,P}}{f_{,M}} + (E_p I)\frac{f_{,M}}{f_{,P}} \right] d\delta_p < 0 \tag{45}$$

or

$$dM < -\frac{f_{,P}}{f_{,M}} dP.$$

It is seen that eqns (44) and (45) are exactly the plastic flow conditions formulated in Section 4.2 for a work-hardening material.

4.7. *Calculation of the plastic modulus history curve*

The plastic modulus is recognised as the key parameter in describing material behaviour under stress reversals. There are several possible forms for the analytical function of E_p. The models, based on the bounding surface plasticity model (Dafalias and Popov, 1976; Tseng and Lee, 1983), typically accept the following form:

$$E_p = E_p^0 + h\left(\frac{\delta}{\delta_{ini} - \delta}\right) \tag{46}$$

where h is the positive shape parameter; δ is the difference between the stress point on the loading surface and the matching point on the bounding surface; δ_{ini} is the distance between the two previous points when the plastic loading initiates; E_p and E_p^0 are the plastic moduli corresponding to the yield surface and the bounding surface, respectively.

The analytical expression for plastic modulus, proposed in this model, is based on the tangent modulus idealisation curves (Fig. 4) and is given by:

$$E_p = h\frac{EE_t}{E - E_t} \tag{47}$$

in which h is the shape calibration parameter, which can be determined through the experiment made on the brace members under cyclic loading, and for a given value of E. This introduced shape calibration parameter accounts for: the linear idealised nature of the tangent modulus history model; the idealised representation of the yielding zone as the hinge point at the midspan; etc. The plastic modulus history as compared to the tangent modulus history is shown in Fig. 7. One can observe that for $E_t = E$, E_p approaches infinity (i.e. as is expected for elastic behaviour), and the plastic modulus values decrease monotonically as the tangent moduli and axial forces decrease continuously, thus satisfying the necessary conditions.

It must be noted that the proposed model, as distinct from the previous models, is capable of accounting for the deterioration of the tangent modulus through variation of the value of P_y, in accordance with the hardening rules used. The result is that the curves are not stable any longer; and the same is true for the plastic modulus curves. It is believed that the models for the tangent modulus history and the plastic modulus history presented in this manner will better represent the analytical prediction of the cyclic behaviour of a brace member.

In Fig. 7(a), two idealised tangent and plastic modulus curves are shown. The plastic modulus curve is derived by the use of eqn (47). In order to verify this curve, it was derived analytically from the experimental data (Leowardi 1994).

This verification involved the following steps:

(1) From eqn (42), we get

$$\frac{E_p}{E} = \frac{\Delta M + \dfrac{f_{.P}}{f_{.M}}\Delta P}{\left[(EA)\dfrac{f_{.P}}{f_{.M}} + (EI)\dfrac{f_{.M}}{f_{.P}}\right]\Delta\delta_p} \tag{48}$$

where ΔP and ΔM are the increments of axial load and plastic hinge moment from experimental data.

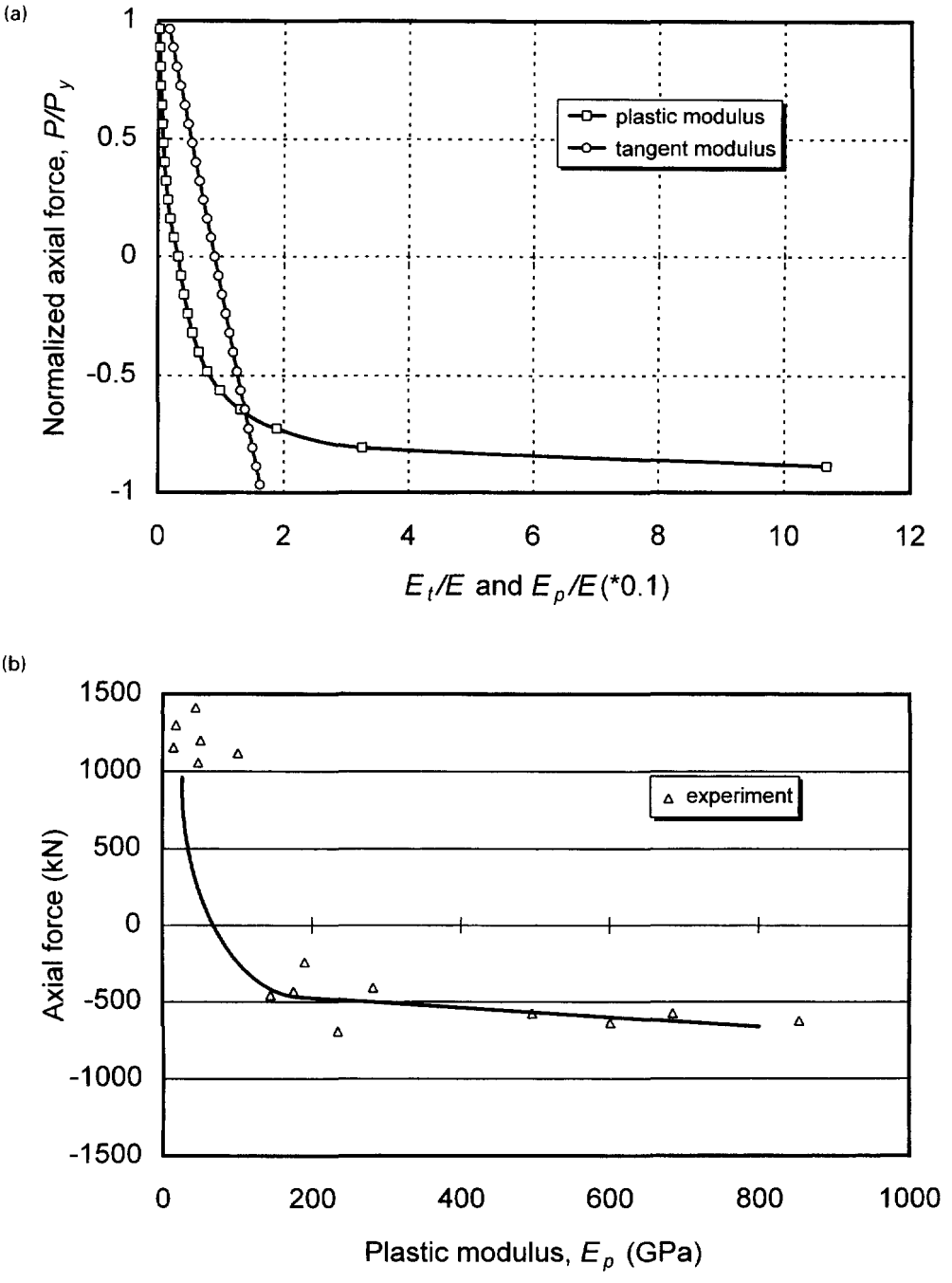

Fig. 7. Tangent and plastic modulus histories: (a) analytical models; (b) plastic modulus values via experiment.

(2) The increment $\Delta\delta_p$ can be derived from eqn (11)

$$\Delta\delta_p = \frac{f_{,P}}{f_{,M}} \frac{d\Phi_p}{dP} \Delta P \tag{49}$$

in which $d\Phi_p/dP$ is defined by eqn (40).

(3) The relative plastic hinge rotation can be evaluated from the equilibrium condition

$$\Phi_i = \frac{M_i}{\gamma(v_i) E_t I} \tag{50}$$

where v_i, M_i and Φ_i are determined at the current stress point.

A scatter plot which shows the joint distribution of axial force and plastic modulus, is depicted in Fig. 7(b). The trendline, calculated by the least squares fit, displays the trend of the plastic modulus behaviour, which is similar to the trend shown in Fig. 7(a).

5. MODELLING OF WORK-HARDENING EFFECTS FOR A BRACE MEMBER

5.1. *Hardening rules*

The existing and widely-used plasticity models differ from each other in their use of the hardening rules which specify the modification of the yield condition during the course of plastic deformation. To characterise the observed phenomena in the cyclic material behaviour, the yield surface and the fully plastic interaction curve can be allowed to expand (isotropic hardening) and/or translate (kinematic hardening) in the stress resultant space. Within the scope of this paper, the simplest hardening rules are employed. The motion of the yield surface can be either in the direction of plastic strain rate (Prager's Rule), in the direction of the vector connecting the centre of the yield surface to the current load point (Ziegler's Rule), or in the direction of the stress increment (Phillips' Rule).

5.2. *Experimental observations*

The phenomenon of cyclic strain hardening was observed experimentally for all specimens tested (Leowardi, 1994). The cycle-by-cycle comparison of the theoretical fully plastic P–M curve and the P–M interaction curves obtained experimentally is shown in Fig. 8. As one can see, in the earlier cycles, the experimental P–M interaction curves tended to follow the fully plastic theoretical curve. After the fourth cycle, both specimens demonstrated rapid buckling load deterioration along with the increase in the maximum tensile load capacity and in the value of the fully plastic moment M_p. During the later cycles, both struts developed significant strain hardening, as represented by shifts in the experimental P–M curves. The signs of strain softening in the compression side during the later cycles can also be seen.

The increase in values of the experimental maximum tensile load and the fully plastic moment from cycle to cycle supports the trend that the yield surface expands isotropically in the stress resultant space. On the other hand, the deterioration in the buckling load from cycle to cycle clearly indicates the presence of the Bauschinger effect upon reverse loading;

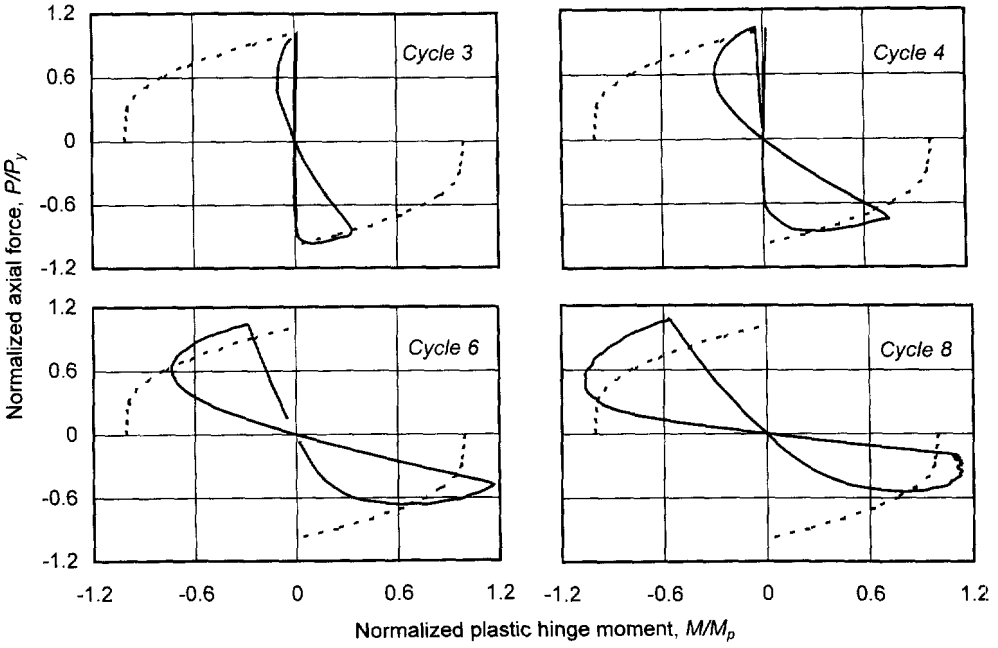

Fig. 8. Comparison of fully plastic and experimental P–M interaction curves.

but, purely isotropic hardening is not associated with any direction of loading; thus, it is one of the less suitable models for stress reversals with the Bauschinger effect.

Since all hardening rules are of phenomenological nature and were derived from the experimental observations on specimens different from brace members, the verification of the computation models against the experimental data has to be performed with an emphasis on how to describe the change of the yield surface for a brace member under stress reversals.

5.3. *Purely kinematic hardening*

In this section specific kinematic hardening rules are considered, and their capability to describe the hardening phenomena with regard to the brace cyclic behaviour is evaluated.

Prager's kinematic rule. If the Prager's hardening rule (Prager, 1956) is used to determine the parameter $\{\alpha\}$, then the incremental movement of the subsequent yield surface centre can be calculated as follows:

$$d\alpha_P = f_{,P}\frac{f_{,P}\,dP + f_{,M}\,dM}{f_{,P}^2 + f_{,M}^2},$$
$$d\alpha_M = f_{,M}\frac{f_{,P}\,dP + f_{,M}\,dM}{f_{,P}^2 + f_{,M}^2}. \tag{51}$$

From Fig. 9, it can be seen that the shifts of the interaction curve in the direction of axial force are so negligible that it moves practically along the M-axis only. It results, on the one hand, in an increase in buckling load capacity and, on the other hand, in a decrease in maximum tensile load capacity [Fig. 10(a)]. As for the interaction curve in this case, one can see a significant decrease in the developed plastic hinge moment in the tension side [Fig. 10(b)]. For that reason, the results obtained by the use of this hardening rule contradict the experimentally observed expansion of the interaction curve in both the positive and negative direction of plastic hinge moment.

Phillips' kinematic rule. Experimental results, reported by Phillips and Lee (1977), indicated a translation of the yield surface along the direction of the stress increment. In

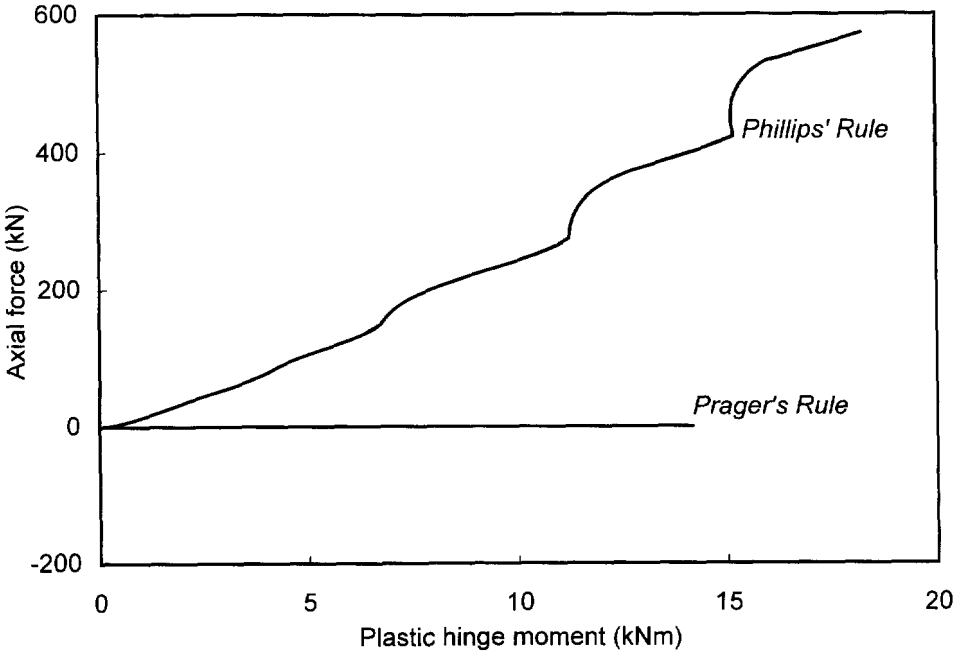

Fig. 9. Yield surface centre locus for different hardening rules.

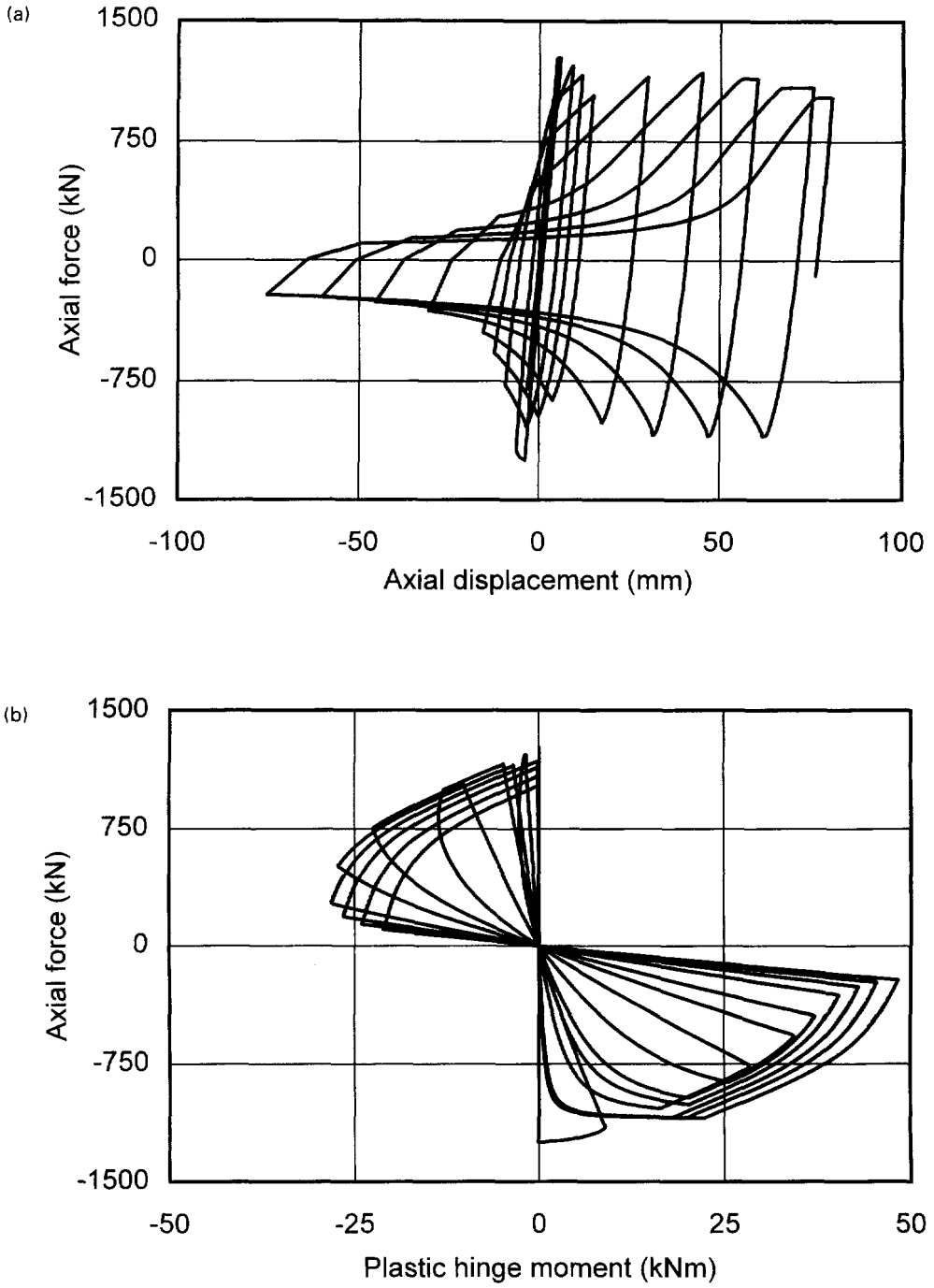

Fig. 10. Effect of kinematic hardening (Prager's rule): (a) P–δ curve; (b) P–M curve.

this case, the following simple expressions for the incremental motion of the yield surface can be derived as:

$$d\alpha_P = dP,$$
$$d\alpha_M = dM. \tag{52}$$

It is worth noting that the increments dP and dM are always of positive sign during the course of plastic deformation. Because of this, eqn (52) predicts the motion of the yield surface upward as seen in Fig. 9. The resulting axial force–axial displacement curve for a

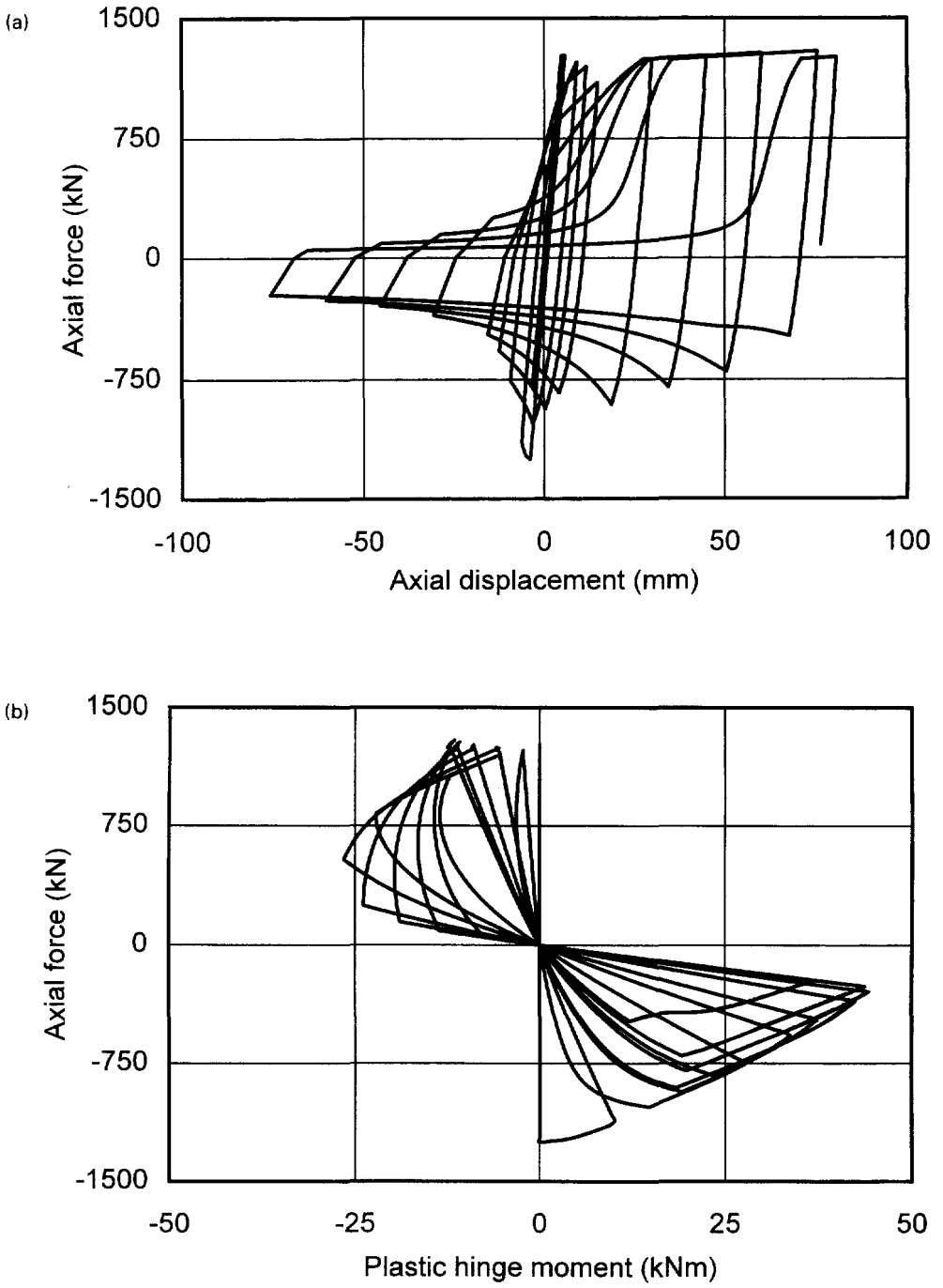

Fig. 11. Effect of kinematic hardening (Phillips's rule): (a) P–δ curve; (b) P–M curve.

double fixed specimen is shown in Fig. 11(a). One can see that, in the compression side, the cyclic behaviour of a brace member is modelled well including the deterioration in buckling load, but there is nothing like strain hardening in the tension side.

5.4. *Independent and mixed hardening rules*

From the comparison presented above, it may be concluded that neither of the considered simple kinematic hardening plasticity models is able to predict the true behaviour of a brace member. Whereas the purely isotropic hardening model is capable of predicting the expansion of the yield surface, it failed to represent the Bauschinger effect exhibited by steel. On the other hand, the Baushinger effect can be handled by the use of the kinematic

hardening rule. There is evidently a strong case for a combination of kinematic and isotropic hardening, i.e. a mixed hardening rule, as well as for introducing an independent hardening rule, which states that the direction of the motion of yield surface under a tension loading and under a compression loading are independent of each other.

The isotropic hardening rule states that the progressively increasing yield stresses under both tension and compression loading are always the same. The relationship between the hardening parameter κ and the accumulated plastic strain $\tilde{\varepsilon}_p$, which characterises the hardening process of a material, has been calibrated on the uniaxial cyclic stub column stress test (Remennikov and Walpole, 1995). The function used to define the hardening parameter κ is based on one of the fully cycled curves and has the following form:

$$\kappa = h_p \times (\tilde{\varepsilon}_p) + f_y \tag{53}$$

in which f_y is the nominal yield stress of the material, and h_p is the calibration parameter ($h_p = 6875$ is used here).

The independent hardening rule is introduced in this report to reflect the hardening phenomena observed during the tests on the brace members. As detailed earlier, the stress resultant increments dP and dM retain their positive values over a course of plastic loading. This fact consequently causes the motion of yield surface predominantly in one direction. To better represent the strain hardening effect for the brace members cyclic behaviour, it is proposed to introduce two different hardening rules under a tension loading and under a compression loading. Taking the Phillips' hardening rule eqn (52) as the basis for further development, the proposed modification takes the following form

$$\begin{aligned} &\text{For tension } d\alpha_P = dP, \quad \text{and for compression } d\alpha_P = dP, \\ &d\alpha_M = -dM \qquad\qquad d\alpha_M = dM. \end{aligned} \tag{54}$$

It is expected that the proposed modification will improve the prediction of the strain hardening effect both in the tension and compression side, since it allows for the yield surface moving so that both the strain hardening in tension and the Baushinger effect can be modelled.

A combination of isotropic and kinematic hardening allows the yield surface to expand and translate simultaneously in stress resultant space. The total increment of plastic deformation can be split into two collinear vectors:

$$d\{\varepsilon^p\} = d\{\varepsilon^p_{is}\} + d\{\varepsilon^p_k\} \tag{55}$$

where $d\{\varepsilon^p_{is}\}$ is associated with the expansion of the yield surface (isotropic hardening) and $d\{\varepsilon^p_k\}$ is associated with the translation of the yield surface (kinematic hardening).

If we assume that the contribution of each term to the total plastic deformation increment is constant over the course of loading, then there exists a weighting coefficient, W, such that these two components can be written as follows:

$$\begin{aligned} d\{\varepsilon^p_{is}\} &= W\, d\{\varepsilon^p\}, \\ d\{\varepsilon^p_k\} &= (1-W)\, d\{\varepsilon^p\} \end{aligned} \tag{56}$$

in which W is within the range $0 < W \leqslant 1$. With the mixed hardening rule, different degrees of the Bauschinger effect can be simulated by adjusting the two hardening parameters, κ and $\{\alpha\}$, which define the size and position of the yield surface.

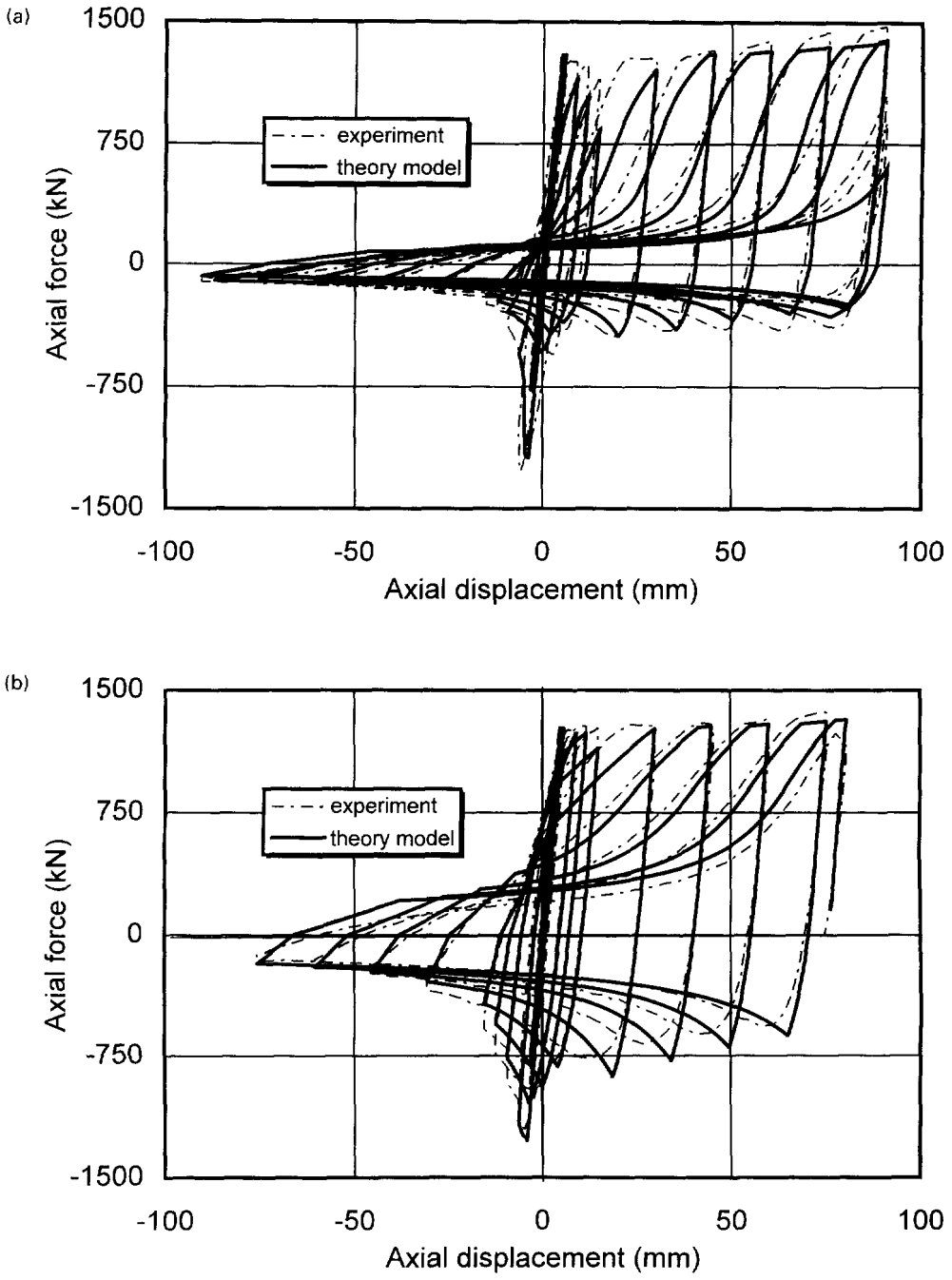

Fig. 12. Comparison of analytical (with mixed hardening) and experimental P–δ curves: (a) pinned–pinned brace member; (b) fixed–fixed brace member.

Figure 12 shows the result of using the independent and mixed hardening rules for predicting behaviour of specimens with different boundary conditions under cyclic loading. The presence of all phenomena mentioned above can be recognised. As one can see, in both cases the implemented hardening rules enabled the model to simulate the shifts of yield surface during later cycles in tension, the increase in the value of M_p in compression, as well as the deterioration in the buckling load with cycling.

6. SUMMARY AND CONCLUSIONS

Some previous analytical models for simulating the cyclic inelastic behaviour of steel bracing members have been reviewed. Based on this review, it appears that existing physical

theory brace models fail to account for certain behaviour phenomena. Most of these models assume elastic–perfectly plastic material properties. This results in inaccurate analytical predictions of member behaviour. None of these models, therefore, can account for the following features: (1) the Bauschinger effect; (2) local buckling; (3) the gradual spread of plastification along the length of the brace member. In addition, existing physical theory brace models express axial displacement as a function of axial force. Thus, these models require additional iterations to estimate the value of the axial force for a given displacement, when being used in conjunction with the matrix displacement method to analyse a real structure. An incremental physical theory model has been developed herein to address these problems.

A plasticity model in stress–resultant space was developed in order to describe work-hardening phenomena observed during an experimental program made on the different types of brace members. The explicit expressions for components of a plastic strain vector were presented in an incremental form. This enables the inclusion of the plastic deformation increment for work-hardening material into the incremental physical theory brace model to account for the work-hardening effects.

To ensure the plastic flow takes place under cyclic loading, the loading/unloading criterion, which takes into consideration some features of the brace member behaviour, was formulated. The formulae for the plastic hinge moment increment, which satisfies the plastic loading criterion both in Zone P1 and Zone P2, were derived from the formula for the axial plastic deformation for work-hardening material.

The plastic modulus, E_p, is recognised as the key parameter in evaluating material behaviour under stress reversals. An analytical expression, which relates the plastic modulus, E_p, to the elastic modulus, E, and the tangent modulus, E_t, was proposed. The tangent modulus model was that proposed by Ikeda and Mahin (1984) for the refined physical theory brace model.

To study the observed phenomena in the cyclic material behaviour, several hardening rules of the one-surface type were employed to evaluate the effect on the analytical P–δ and P–M curves. The comparison revealed that neither of the considered simple hardening plasticity models was able to predict the true behaviour of a brace member under cyclic loading. Then, some modifications were proposed to the Phillips' hardening rule and the mixed hardening rule was introduce to better represent the analytical prediction of a brace member cyclic phenomena. These hardening rules were implemented into the quasi-static computer program "BRACE MODEL" and computer studies made on the brace members demonstrated that the incremental physical theory brace model was able to represent cyclic buckling behaviour very effectively. In addition, this model has been incorporated into the inelastic dynamic frame analysis program "RUAUMOKO" (Carr, 1996) in order to enable evaluation of the inelastic seismic response of the steel braced structures.

Acknowledgements—This research was funded by a grant from the New Zealand Foundation for Research, Science and Technology for the first author. This support is sincerely appreciated. Thanks also go to the anonymous reviewers for their valuable comments on this study.

REFERENCES

Ballio, G. and Perotti, F. (1987). Cyclic behaviour of axially loaded members; numerical simulation and experimental verification. *Journal of Constructional Steel Research* **7**, 3–41.

Black, R. G., Wenger, W. and Popov, E. P. (1980). Inelastic buckling of steel strut under cyclic load reversals. EERC Report No. 80/40, Earthquake Engineering Research Center, University of California, Berkeley, CA.

Carr, A. J. (1996). "RUAUMOKO". Computer Program Library, Department of Civil Engineering, University of Canterbury, New Zealand.

Chen, W. F. and Atsuta, T. (1977). *Theory of Beam-Columns*, Vol. 2, *Space Behaviour and Design*. McGraw-Hill, New York.

Chen, W. F. and Han, D. J. (1988). *Plasticity for Structural Engineers*. Springer, New York.

Dafalias, Y. F. and Popov, E. P. (1976). Plastic internal variables formalism in cyclic plasticity. *Journal of Applied Mechanics* **98**, 645–651.

Drucker, D. C. (1960). Plasticity. In *Structural Mechanics*, pp. 407–488. Pergamon Press, London.

Gugerli, H. and Goel, S. C. (1982). Inelastic cyclic behaviour of steel bracing member. Report No. 82R1, Department of Civil Engineering, University of Michigan, Ann Arbor.

Higginbotham, A. (1973). The inelastic cyclic behaviour of axially-loaded steel members. Ph.D. Thesis, University of Michigan, Ann Arbor.
Ikeda, K. and Mahin, S. A. (1984). A refined physical theory model for predicting the seismic behavior of braced steel frames. EERC Report No. 84/12, Earthquake Engineering Research Center, University of California, Berkeley, CA.
Jain, A. K. and Goel, S. C. (1978). Hysteresis models for steel members subjected to cyclic buckling or cyclic end moments and buckling. UMEE Report No. 78R6, University of Michigan, Ann Arbor.
Jiang, Y. and Sehitoglu, H. (1996). Comments on the Mroz multiple surface type plasticity models. *International Journal of Solids and Structures* **33,** 1053–1068.
Kayvani, K. and Barzegar, F. (1996). Hysteretic modelling of tubular members and offshore platforms. *Engineering Structures* **18,** 93–101.
Leowradi, L. S. (1994). Performance of steel brace members. ME Thesis, University of Canterbury, Christchurch, New Zealand.
Maison, B. and Popov, E. P. (1980). Cyclic response prediction for braced steel frames. *Structural Division, ASCE* **106,** 1401–1416.
Mroz, Z. (1983). Hardening and degradation rules for metals under monotonic and cyclic loading. *Journal of Engineering Materials Technology, ASME* **105,** 113–118.
Nilforoushan, R. (1973). Seismic behaviour of multi-storey K-braced frame structures. UMEE Report No. 73R9, University of Michigan, Ann Arbor.
Nonaka, T. (1973). An elastic–plastic analysis of a bar under repeated axial loading. *International Journal of Solids and Structures* **9,** 569–580.
Nonaka, T. (1977). Approximation of yield condition for the hysteric behaviour of a bar under repeated axial loading. *International Journal of Solids and Structures* **13,** 637–643.
Orbison, J. G., McGuire, W. and Abel, J. F. (1982). Yield surface applications in non-linear steel frame analysis. *Computational Methods in Applied Mechanical Engineering* **33,** 557–573.
Phillips, A. and Lee, C. W. (1977). Yield surfaces and loading surfaces. Experiments and recommendations. *International Journal of Solids and Structures* **15,** 715–729.
Prager, W. (1956). A new method of analyzing stress and strains in work-hardening solids. *Journal of Applied Mechanics, ASME* **23,** 493–396.
Remennikov, A. M. and Walpole, W. R. (1995). Incremental model for predicting the inelastic hysteretic behaviour of steel bracing members. Research Report 95-6. Department of Civil Engineering, University of Canterbury, Christchurch, New Zealand.
Remennikov, A. M. and Walpole, W. R. (1996). Analytical prediction of cyclic behaviour for steel braced frames. *Proc. NZNSEE Conference*, pp. 211–218. New Plymouth, New Zealand.
Shibata, M. (1982). Analysis of elastic–plastic behaviour of a steel brace subjected to repeated axial force. *International Journal of Solids and Structures* **18,** 217–228.
Singh, P. (1977). Seismic behaviour of braces and braced steel frames. Ph.D. Thesis, University of Michigan, Ann Arbor.
Tseng, N. T. and Lee, G. C. (1983). Simple plasticity model of two-surface type. *Journal of the Engineering Mechanics Division, ASCE* **109,** 795–810.
Walpole, W. R. (1995). Behaviour of cold-formed steel RHS members under cyclic loading. *Proceedings of the NZNSEE Conference*, pp. 70–75. Rotorua, New Zealand.
Ziegler, H. (1959). A modification of Prager's hardening rule. *Quarterly Appl. Mat.* **17,** 55–65.

APPENDIX

An interaction curve for the initial yielding may serve as a yielding function for the cross section in the absence of residual stresses. A single, as well as continuous function for structural steel was obtained by Orbison *et al.* (1982). The exact interaction curves for the 150UC30 section are depicted in Fig. A1. The step wise regression analysis was carried out making use of the data from Fig. A1. The modified function, which best fits the exact solution data for the 150UC30 section, now takes the following form

$$p^2 + m_x^2 + m_y^4 + 4.05p^2m_x^2 + 8.26p^6m_x^2 + 3.68p^6m_y^2 + 10.4p^6m_y^4 + 4.65m_x^4m_y^2 = 1 \tag{A.1}$$

where $p = P/P_y$ = normalised axial force; $m_x = M_x/M_{px}$ = normalised strong axis bending moment; and $m_y = M_y/M_{py}$ = normalised weak axis bending moment.

The comparison of the approximated and exact solutions is shown in Fig. A1. It is seen that eqn (A1) is in good agreement with the plastification values. The correlation is particularly good for both the axial force–strong axis bending interaction and the axial force–weak axis bending interaction. Taking into account either the effect of weak axis bending or the effect of strong axis bending, formula (A1) can be reduced to the following equations

$$p^2 + m_y^4 + 3.68p^6m_y^2 + 10.4p^6m_y^4 = 1, \tag{A.2}$$

$$p^2 + m_x^2 + 4.05p^2m_x^2 + 8.26p^6m_x^2 = 1. \tag{A.3}$$

In this paper, eqn (A2) was used as the yield surface f for evaluation of the plastic deformation of a brace member under an out-of-plane inelastic buckling.

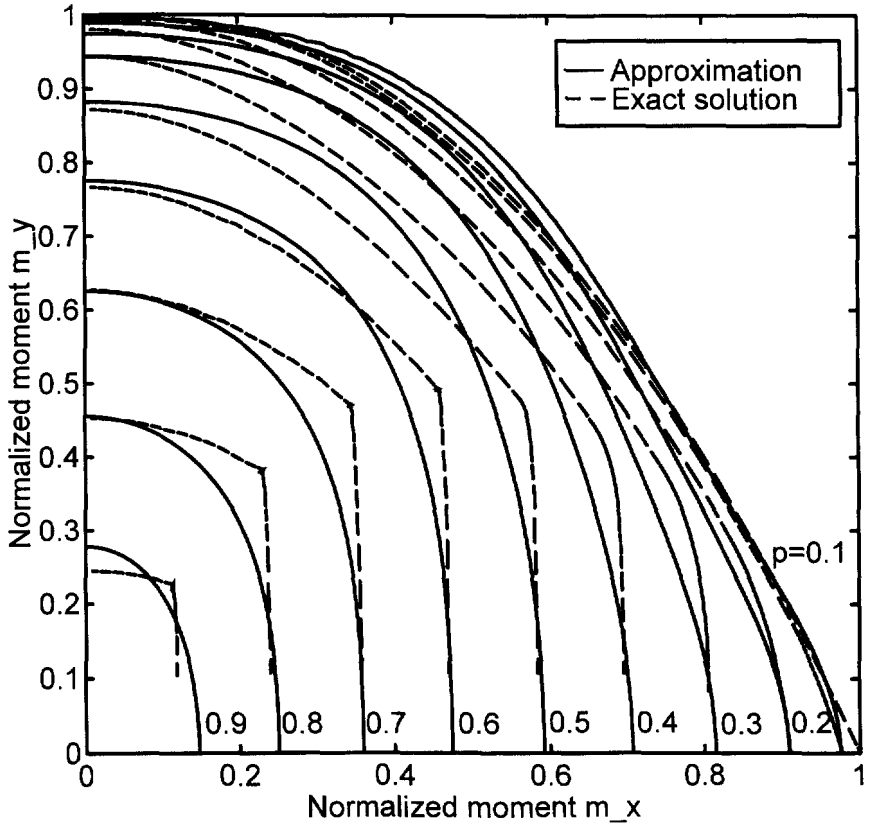

Fig. A1. Bi-axial interaction curves for 150UC30 section.